

Convergence Analysis for Turbo Trellis Coded Modulation

Hangjun Chen and Alexander Haimovich
 Department of Electrical and Computer Engineering
 New Jersey Institute of Technology
 Newark, NJ 07102
 {hxc1170, haimovic}@njit.edu

Abstract—In this paper we extend the previously proposed extrinsic information exchange charts (EXIT) method for the analysis of the convergence of turbo codes to turbo coded modulation (TTCM) schemes. The effectiveness of the proposed method is demonstrated through examples. The proposed method provides a convenient way to systematically compare between schemes and thus can be used as a tool in the design of TTCM.

I. INTRODUCTION

Convergence analysis of iterative decoding algorithms for turbo codes has received much attention recently due to its useful application to predicting code performance, its ability to provide insights into the encoder structure, and its usefulness in helping with the code design. Several methods have been proposed to analyze the convergence of the iterative decoders for binary turbo codes [1], [2], [3]. In particular, the extrinsic information transfer (EXIT) method [1] has created a lot of interest. The EXIT method has been extended to the analysis of nonbinary turbo codes in [4].

Turbo trellis coded modulation (TTCM) [5], [6], conjoins signal mapping techniques, such as Ungerboeck's signal space partition, with turbo coding, to achieve significant coding gains without increasing bandwidth. However the need for signal mapping makes the encoder structure more complex to design and analyze than binary turbo codes. Hence the convergence analysis is a very important tool for the design and comparison between TTCM schemes.

In TTCM, the systematic bits and parity bits are usually mapped to and transmitted as a single symbol. At the receiver, a symbol decoder is used instead of a binary decoder [5], [6]. Consequently, the systematic information and extrinsic information are not naturally separated as in binary turbo codes. The separation is not necessary for carrying out the decoding. It is however, needed for generating the EXIT chart. Due to the mixing of the systematic and extrinsic information, the approach for generating the EXIT chart for binary decoders, or even for nonbinary decoders [4], can not be directly applied to TTCM.

In this paper, we develop the EXIT chart for TTCM by showing a way to explicitly separate the systematic information and extrinsic information. To be specific, we develop the analysis based on the TTCM codes introduced in [5]. The

application of the proposed method to other structures is fairly straightforward.

The rest of the paper is organized as follows. In section II we briefly introduce the structure of TTCM and we develop the EXIT chart for TTCM in section III. Several examples are used to illustrate and demonstrate the proposed method in section IV. Conclusions are drawn in section V.

II. TTCM STRUCTURE

A. Encoder Structure

The structure of the TTCM encoder [5] is presented in Fig. 1. Assuming 2^{m+1} constellation, at each time interval k , a symbol is transmitted representing m information bits $\mathbf{b}[k] = \{b[k, i]\}_{i=0}^{m-1}$. Of the m bits, possibly only \tilde{m} bits $\{b[k, i]\}_{i=0}^{\tilde{m}-1}$, are encoded, whereas the other $(m - \tilde{m})$ uncoded bits are input directly to the symbol mapper. The turbo encoder consists of two rate $\tilde{m}/(\tilde{m} + 1)$ component recursive systematic convolutional (RSC) encoders, which are connected by a symbol (\tilde{m} bits) interleaver. These \tilde{m} encoded bits, are labeled for later use as the $2^{\tilde{m}}$ -ary level symbol $d[k] \triangleq \sum_{i=1}^{\tilde{m}} b[k, i]2^{i-1}$. The parity bits $c_1[k]$ and $c_2[k]$ from the two component encoders (the parity bits from the encoder with interleaved input are deinterleaved to their original order) are alternatively punctured, and the surviving parity bit $c[k]$ is mapped together with the m data bits to M-QAM or MPSK symbols $s[k]$, and transmitted.

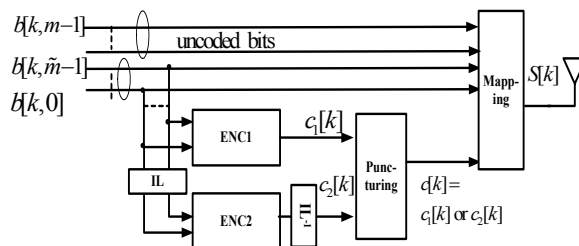


Fig. 1. Structure of TTCM encoder.

B. Decoder Structure

The structure of the TTCM decoder is depicted in Fig. 2. The decoder consists of two symbol maximum *a posteriori* (MAP) decoders, which exchange information about the symbols $\{d[k]\}$ formed by the *encoded* data bits. Of course, no information on uncoded bits is exchanged. Hence in TTCM, the systematic information represents the \tilde{m} coded bits $\{b[k, i]\}_{i=0}^{\tilde{m}-1}$. Let the TTCM codeword consist of N symbols $(s[1], s[2], \dots, s[N])$. The channel observation is given by

$$y[k] = s[k] + n[k], \quad (1)$$

where $n[k]$ is zero mean white Gaussian noise with variance σ^2 . The signal to noise ratio (SNR) is then defined as $E[|s[k]|^2]/\sigma^2$.

Due to fact that the symbol $s[k]$ embodies both the systematic and parity bits, and consequent to the alternative puncturing of the parity bits, it is shown in [5] that half of the information exchanged between component decoders contains systematic information and half does not. Unlike the binary turbo code case, the *a posteriori* probabilities (APP) $\mathbf{L}_p[k] \triangleq \{\log P(d[k] = u|\mathbf{y})\}_{u=0}^{2^{\tilde{m}}-1}$ computed by either component decoder can only be decomposed into two parts. The first part is the *a priori* input $\mathbf{L}_a[k] \triangleq \{\log P(d[k] = u)\}_{u=0}^{2^{\tilde{m}}-1}$, passed from the other decoder. The second part is different for two cases: (i) at time interval k , $s[k]$ contains the parity bit from the *corresponding* component encoder; (ii) at time interval k , $s[k]$ contains parity bit from the *other* component encoder. For case (ii), the second part only contains the newly generated extrinsic information output, denoted as $\mathbf{L}_e^{out}[k]$. For case (i) however, the second part is a mixture of the extrinsic information and systematic information, denoted as $\mathbf{L}_{es}^{out}[k]$. That is,

$$\mathbf{L}_p[k] = \begin{cases} \mathbf{L}_a[k] + \mathbf{L}_{es}^{out}[k], & k \in \text{case (i)} \\ \mathbf{L}_a[k] + \mathbf{L}_e^{out}[k], & k \in \text{case (ii)} \end{cases}, \quad (2)$$

Accordingly, the *a priori* input to each component decoder $\mathbf{L}_a[k]$ is, for case (i), only extrinsic information, denoted as $\mathbf{L}_e^{in}[k]$; and is, for case (ii), the mixture of both extrinsic information and systematic information, denoted as $\mathbf{L}_{es}^{in}[k]$. That is

$$\mathbf{L}_a[k] = \begin{cases} \mathbf{L}_e^{in}[k], & k \in \text{case (i)} \\ \mathbf{L}_{es}^{in}[k], & k \in \text{case (ii)} \end{cases}. \quad (3)$$

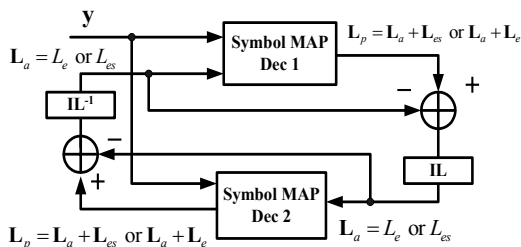


Fig. 2. Structure of TTCM decoder.

III. EXIT CHARTS FOR TTCM

The EXIT chart is a tool for studying the convergence of turbo decoders without simulating the whole decoding process. The chart is generated by a single component decoder by mimicking the *a priori* input (as if it is generated by the other decoder) and measuring the output. It was found in [1], [2], [3] that for binary MAP decoders, when the random interleaving sufficiently deep, the *a priori* inputs (the extrinsic information passed from the other component decoder), $\lambda = \log \frac{P(b=1)}{P(b=0)}$, for each data bit b , are mutually independent and can be closely modeled as independent, identically distributed (i.i.d.) random variables that follow the same Gaussian distribution $p(\lambda|b)$. In addition, the mean value μ and variance σ^2 of $p(\lambda|b)$ satisfy the consistency condition $\mu = \frac{1}{2}\sigma^2$. Note now $p(\lambda|b)$ is determined by only one parameter, either μ or σ^2 . So to generate λ with a given mutual information content $A = I(\lambda; b)$, the parameter of $p(\lambda|b)$, μ (or σ^2) can be found by

$$\begin{aligned} A &= I(\lambda; b) \\ &= \frac{1}{2} \sum_{x=0,1} \int_{-\infty}^{+\infty} p(\lambda|b=x) \\ &\quad \cdot \log \frac{2 \cdot p(\lambda|b=x)}{p(\lambda|b=0) + p(\lambda|b=1)} d\lambda \\ &\triangleq J(\mu) \end{aligned} \quad (4)$$

and

$$\mu = J^{-1}(A). \quad (5)$$

The above procedure is used to generate the *a priori* input to a binary MAP decoder. For TTCM, the component decoder is a nonbinary symbol decoder, and the *a priori* has different contents in actual operation for the two different cases shown in (3). To mimic the *a priori* input $\mathbf{L}_e^{in}[k]$ for $k \in \text{case (i)}$, which contains only the extrinsic information generated by the other decoder, we adopt the assumption proposed in [4] that the log-likelihood ratios $\{\lambda[k, i] = \log \frac{P(b[k, i]=1)}{P(b[k, i]=0)}\}_{i=0}^{\tilde{m}-1}$ for the bits $\{b[k, i]\}_{i=0}^{\tilde{m}-1}$ composing the nonbinary symbol $d[k]$ are i.i.d. Gaussian random variables. Thus $\{\lambda[k, i]\}_{i=0}^{\tilde{m}-1}$ can be generated as in the binary turbo code case, with the value A in (5) is set to $A = I_e^{in}/\tilde{m}$, where I_e^{in} is the desired mutual information between $\mathbf{L}_e^{in}[k]$ and $d[k]$, i.e., $I_e^{in} = I(\mathbf{L}_e^{in}[k]; d[k])$. The term $\mathbf{L}_{es}^{in}[k] = \{\log P(d[k] = u)\}_{u=0}^{2^{\tilde{m}}-1}$ can be calculated using $\{\lambda[k, i]\}_{i=0}^{\tilde{m}-1}$.

For $k \in \text{case (ii)}$, the *a priori* is a mixture of both extrinsic and systematic information $\mathbf{L}_{es}^{in}[k]$ as shown in (3). Before generating the mixture, we need to find out what the systematic information would be, even it does not appear explicitly during the decoding process in TTCM. In binary turbo coding, the systematic information is the information associated with the channel observation of the systematic bit. This should also be the case in TTCM, although each sample of the channel observation contains both systematic bits (symbol), uncoded bits and parity bits. That is, the systematic information about symbol $d[k]$ should be computed as in (6), which is shown at the bottom of next page.

We can also rewrite (6) in the form of vector of log-likelihood values as

$$\mathbf{L}_s[k] = \{\log P(d[k] = u|y[k]), u = 0, \dots, 2^{\tilde{m}} - 1\} \quad (7)$$

We have now explicitly formed the systematic information $\mathbf{L}_s[k]$, for $k \in \text{case (ii)}$. To generate the mixture, we also generate for each $k \in \text{case (ii)}$ a vector extrinsic part $\mathbf{L}_e^{in}[k]$ with $I(\mathbf{L}_e^{in}[k]; d[k]) = I_e^{in}$, in the same way as for case (i). And the mixture $\mathbf{L}_a[k] = \mathbf{L}_{es}^{in}[k]$ is generated as the combination of extrinsic the information and systematic information, i.e., $\mathbf{L}_a[k] = \mathbf{L}_e^{in}[k] + \mathbf{L}_s[k]$. To conclude, the *a priori* input to the TTCM component decoder is generated as

$$\mathbf{L}_a[k] = \begin{cases} \mathbf{L}_e^{in}[k], & k \in \text{case (i)} \\ \mathbf{L}_e^{in}[k] + \mathbf{L}_s[k], & k \in \text{case (ii)} \end{cases} \quad (8)$$

We turn now to the measurement of the extrinsic information at the output of the TTCM component decoder. According to (2), for $k \in \text{case (i)}$ the extrinsic information is mixed with systematic information. However, we can form the systematic information using (6) and (7) and subtract it. That is, the extrinsic information $\mathbf{L}_e^{out}[k]$ for data symbol $d[k]$ is obtained as:

$$\mathbf{L}_e^{out}[k] = \begin{cases} \mathbf{L}_p[k] - \mathbf{L}_a[k] - \mathbf{L}_s[k], & k \in \text{case(i)} \\ \mathbf{L}_p[k] - \mathbf{L}_a[k], & k \in \text{case (ii)} \end{cases} \quad (9)$$

Due to the independence assumption, $\{\mathbf{L}_e^{out}[k]\}_{k=0}^{N-1}$ are mutually independent and follow the same distribution $p_e(\mathbf{L}_e^{out}|d)$. The multi-dimensional joint distribution $p_e(\mathbf{L}_e^{out}|d)$ is obtained by measuring the histogram of \mathbf{L}_e^{out} using its samples $\{\mathbf{L}_e^{out}[k]\}_{k=0}^{N-1}$. Then the mutual information between the extrinsic output and the transmitted symbol d is computed as

$$\begin{aligned} I_e^{out} &= I(\mathbf{L}_e^{out}; d) \\ &= \frac{1}{2^{\tilde{m}} - 1} \sum_{u=0}^{2^{\tilde{m}}-1} \int p_e^{out}(\xi|d=u) \cdot \\ &\quad \log \frac{(2^{\tilde{m}} - 1) \cdot p_e^{out}(\xi|d=u)}{\sum_{u=0}^{2^{\tilde{m}}-1} p_e^{out}(\xi|d=u)} d\xi. \end{aligned} \quad (10)$$

The EXIT chart for TTCM is then generated by measuring the output mutual information I_e^{out} as a function of a family of inputs with specified mutual information I_e^{in} and channel observation of specified SNR, $I_e^{out} = f(I_e^{in}, \text{SNR})$.

The overall block diagram for generating EXIT charts for TTCM schemes is illustrated in Fig. 3.

IV. EXAMPLES

In this section, we present a few examples to illustrate the applications of the proposed EXIT chart method for TTCM.

$$\begin{aligned} P(d[k] = u|y[k]) &= \sum_{b[k, \tilde{m}+1]=\{0,1\}} \dots \sum_{b[k, m]=\{0,1\}} \sum_{c[k]=\{0,1\}} P(y[k]|s[k]) = \\ \text{mapping}(d[k] &= u, b[k, \tilde{m} + 1], \dots, b[k, m], c[k]), \quad u = 0, \dots, 2^{\tilde{m}} - 1 \end{aligned} \quad (6)$$

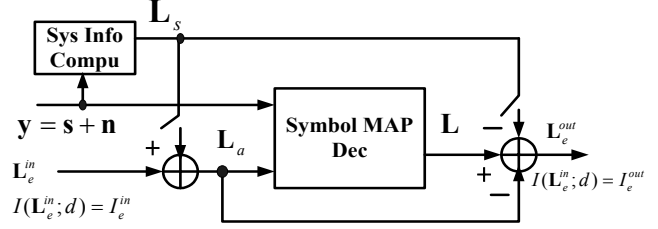


Fig. 3. Block diagram to generate EXIT charts for TTCM schemes.

A. Role of primitive feedback polynomial

We apply the proposed EXIT chart method to analyze and compare two TTCM schemes. The first code is from [5], Table I, first row. This is an 8-state code with 8-PSK modulation, and $m = \tilde{m} = 2$. The second code has the same structure but the parameter $H^0(D)$ in the first row of table I [5] is changed from $(11)_8$ to $(13)_8$. This changes the feedback polynomial of the component encoder from nonprimitive to primitive. Hence, we compare a primitive code and a nonprimitive code.

The EXIT charts for these two codes are presented in Fig. 4, for channel SNR 5.8 dB, 6.2 dB and 7.0 dB, respectively. For schemes with symmetric structure (identical component encoders/decoders), we only need to plot the EXIT chart for one of the decoders. In the figure, the abscissa is $I_e^{in} = I(\mathbf{L}_e^{in}; d)$ in bits, and the ordinate is $I_e^{out} = I(\mathbf{L}_e^{out}; d)$ also in bits.

It is observed from the figure that for both codes, the curves of SNR=5.8 dB intersect with the $y = x$ line, which means that at some point during the iteration the decoder can no longer increase the extrinsic information compared with the input. In this case the decoding will fail no matter how many iterations are run. Both curves for SNR = 6.2 dB are just a little above the $y = x$ line, which means for that any SNR ≥ 6.2 dB, the extrinsic information output at the component decoder will always be better than the input, and the decoder will converge to the correct codeword with high probability. That is, the convergence threshold of these two codes is about 6.2 dB. The simulated bit error rate (BER) performance curve is shown in Fig. 5 after 8 iterations. It is observed that the BER curve actually turns sharply down at about 6.2 dB, which verifies the convergence threshold predicted by the EXIT chart.

In Fig. 4, it is also observed that the curves of the primitive code are always higher than the nonprimitive code, especially at higher values of input mutual information. This implies a faster convergence speed. This agrees with the observation in binary turbo codes that codes with primitive feedback polynomial have faster convergence speed than nonprimitive ones [3]. This observation is also verified by the BER curves in Fig. 5,

where with the same number iterations, the performance of the primitive code is always better than that of the nonprimitive code. So this example suggests that in TTCM primitive codes should be favored over nonprimitive codes.

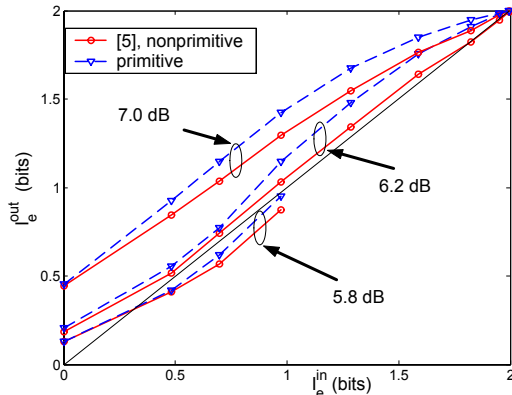


Fig. 4. EXIT charts comparison of two codes.

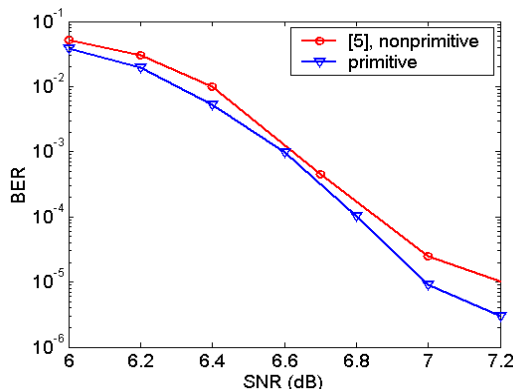


Fig. 5. BER comparison of two codes.

B. Analysis and Design of TTCM Schemes with Uncoded Bits

In this subsection, we first show how to use the proposed EXIT scheme to predict the performance of TTCM schemes with uncoded bits. Then we show how the system design can be improved by examining the EXIT chart.

We study the 3 b/s/Hz, 16 QAM scheme in [5], with 8-state component codes. In this scheme three bits are transmitted at each time interval but only two are coded, consequently there are two parallel branches for each transition in the trellis. The goal of the analysis is to find at what SNR the system can achieve a given bit error rate (BER), e.g., $BER=10^{-5}$. First according to the set partition diagram, [7] Fig. 5, we find that the distance between the parallel transitions is $d_p = \sqrt{8} \cdot \Delta_0$, where Δ_0 is the minimum distance between the points of 16

QAM and $\Delta_0 = 2/\sqrt{10} \cdot E_s$. Since

$$\begin{aligned} BER &= Q\left(\sqrt{\frac{d_p^2}{N_0}}\right) = Q\left(\sqrt{\frac{8\Delta_0^2}{N_0}}\right) \\ &= Q\left(\sqrt{\frac{16E_s}{10N_0}}\right) \end{aligned} \quad (11)$$

the required SNR is

$$\frac{E_s}{N_0} = \frac{10}{16} (Q^{-1}(BER))^2 \quad (12)$$

For $BER=10^{-5}$, the required channel SNR is about 10.5 dB. Next, we generate the EXIT chart for the underlying turbo code at this SNR, which is shown in fig. 7. From the figure it is observed that EXIT curve is far above the $y=x$ line and the opening between the EXIT curve and the $y=x$ line is very large, which means the decoder has converged at $SNR=10.5$ dB and the convergence speed is fast. The convergence threshold for this code is found as 9.6 dB, as also shown in fig. 7. Obviously, the BER performance of the whole system is dominated by the BER of the uncoded bit and the performance of $BER=10^{-5}$ will be achieved at about 10.6 dB. This can be verified by checking the BER performance curve in [5] fig. 9.

The analysis also suggests the turbo code used is too strong, and a code with lower state complexity may be used. In fig. 6 we propose a 4-state component code as an alternative. The EXIT chart for this code is also shown in fig. 7, for $SNR=10.5$ dB. It is observed that although the curve for the 4-state code is lower than the 8-state code, the opening is still very wide and suggests a good convergence speed. Hence, we can lower the complexity of the decoder with little performance loss.

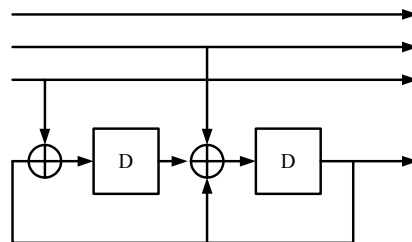


Fig. 6. An alternative 4-state component code for the 3 b/s/Hz, 16QAM scheme.

V. CONCLUSIONS

We have proposed the method to generate the EXIT chart for TTCM decoders. The accuracy and usefulness of this method has been verified through examples. Since the complexity of generating EXIT charts is significantly lower than a full simulation, the proposed method supplies a convenient way to compare between various TTCM schemes as well as to verify and compare between new designs.

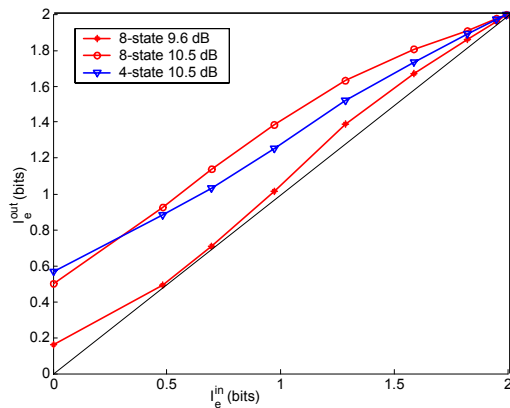


Fig. 7. EXIT charts for two TTCM schemes with 16 QAM, 3 b/s/Hz.

REFERENCES

- [1] S. T. Brink, "Convergence behavior of iterative decoded parallel concatenated codes," *IEEE Transactions on Communications*, vol. 49, pp. 1727–1737, Oct. 2001.
- [2] H. E. Gamal and A. R. Hammons, "Analyzing the turbo decoder using Gaussian approximation," *IEEE Transactions on Information Theory*, vol. 47, pp. 671–686, Feb. 2001.
- [3] D. Divsalar, S. Dolinar, and F. Pollara, "Iterative turbo decoder analysis based on density evolution," *IEEE Journal on Selected Areas in Communications*, vol. 19, pp. 891–907, May 2001.
- [4] A. Grant, "Convergence of non-binary iterative decoding," *GLOBECOM '01*, vol. 2, pp. 1058–1062, Nov 2001.
- [5] P. Robertson and T. Worz, "Bandwidth-efficient turbo trellis-coded modulation using punctured component codes," *IEEE Journal on Selected Areas in Communications*, vol. 16, pp. 206–218, Feb 1998.
- [6] C. Fragouli and R. Wesel, "Turbo-encoder design for symbol-interleaved parallel concatenated trellis-coded modulation," *IEEE Transactions on Communications*, vol. 49, pp. 425–435, March 2001.
- [7] G. Ungerboeck, "Channel coding with multilevel/phase signals," *IEEE Transactions on Information Theory*, vol. 28, pp. 55–67, Jan 1982.